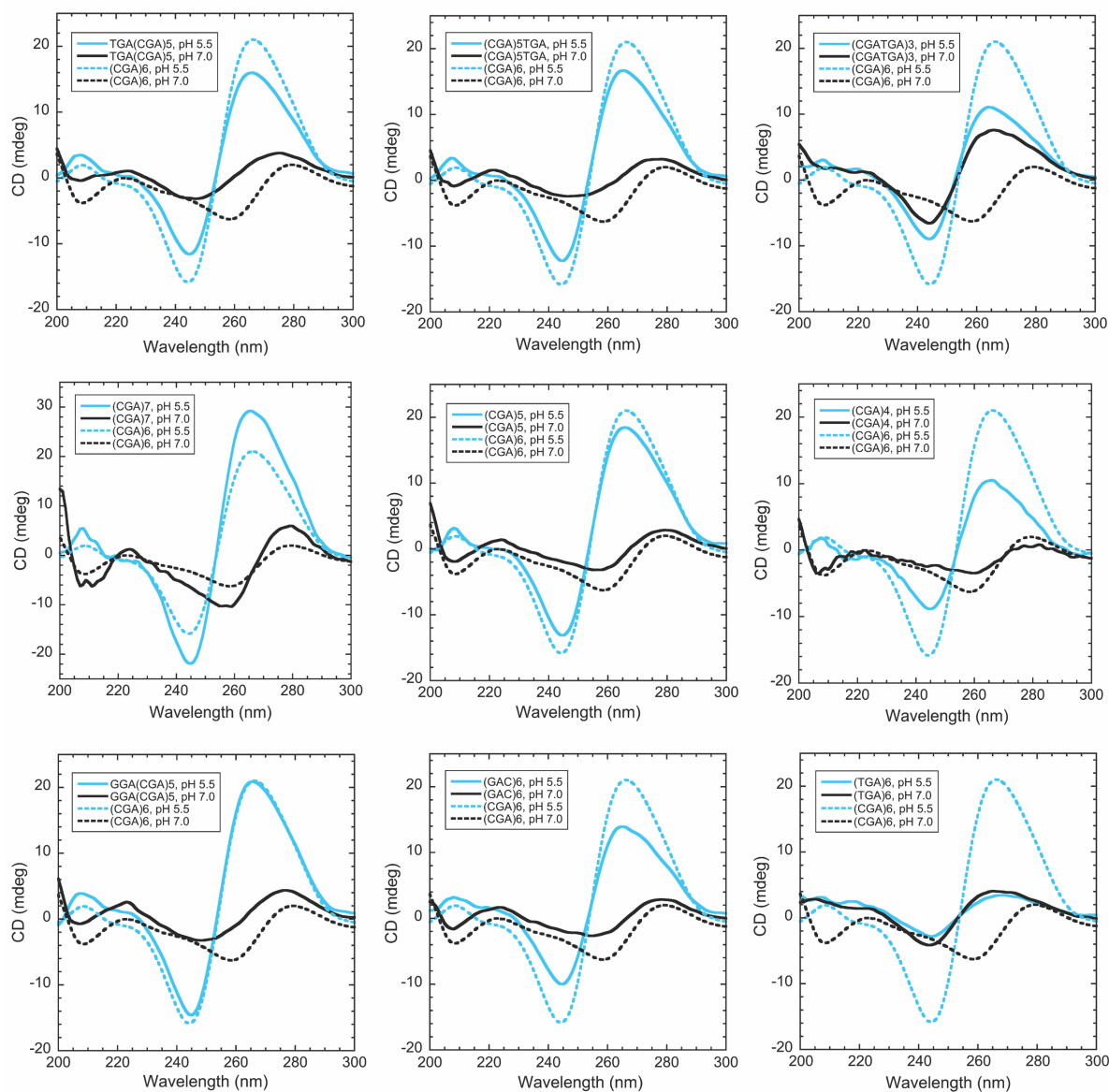


**Biophysical Journal, Volume 119**

**Supplemental Information**

**Stability of the pH-Dependent Parallel-Stranded d(CGA) Motif**

**Emily M. Luteran, Jason D. Kahn, and Paul J. Paukstelis**



**Figure S1.** Circular dichroism spectra of 10  $\mu\text{M}$   $(\text{CGA})_6$  variants. The spectra of  $(\text{CGA})_6$  at pH 5.5 and pH 7.0 are shown (dashed lines) in each panel for reference. At pH 5.5 (blue curves), the prominent positive band at  $\sim 265$  nm and the negative band at  $\sim 245$  nm are characteristic of parallel-stranded duplex formation. As the number of d(CGA) triplets decreases, the intensity of the bands associated with parallel-stranded duplexes also decreases. At pH 7.0 (black curves), the positive band at  $\sim 275$  nm and negative band at  $\sim 258$  nm are characteristic of anti-parallel strands.  $(\text{TGA})_6$  and  $(\text{CGATGA})_3$  have bands characteristic of anti-parallel strands at each pH, suggesting that pH sensitivity is decreased or eliminated with increasing d(TGA) content.

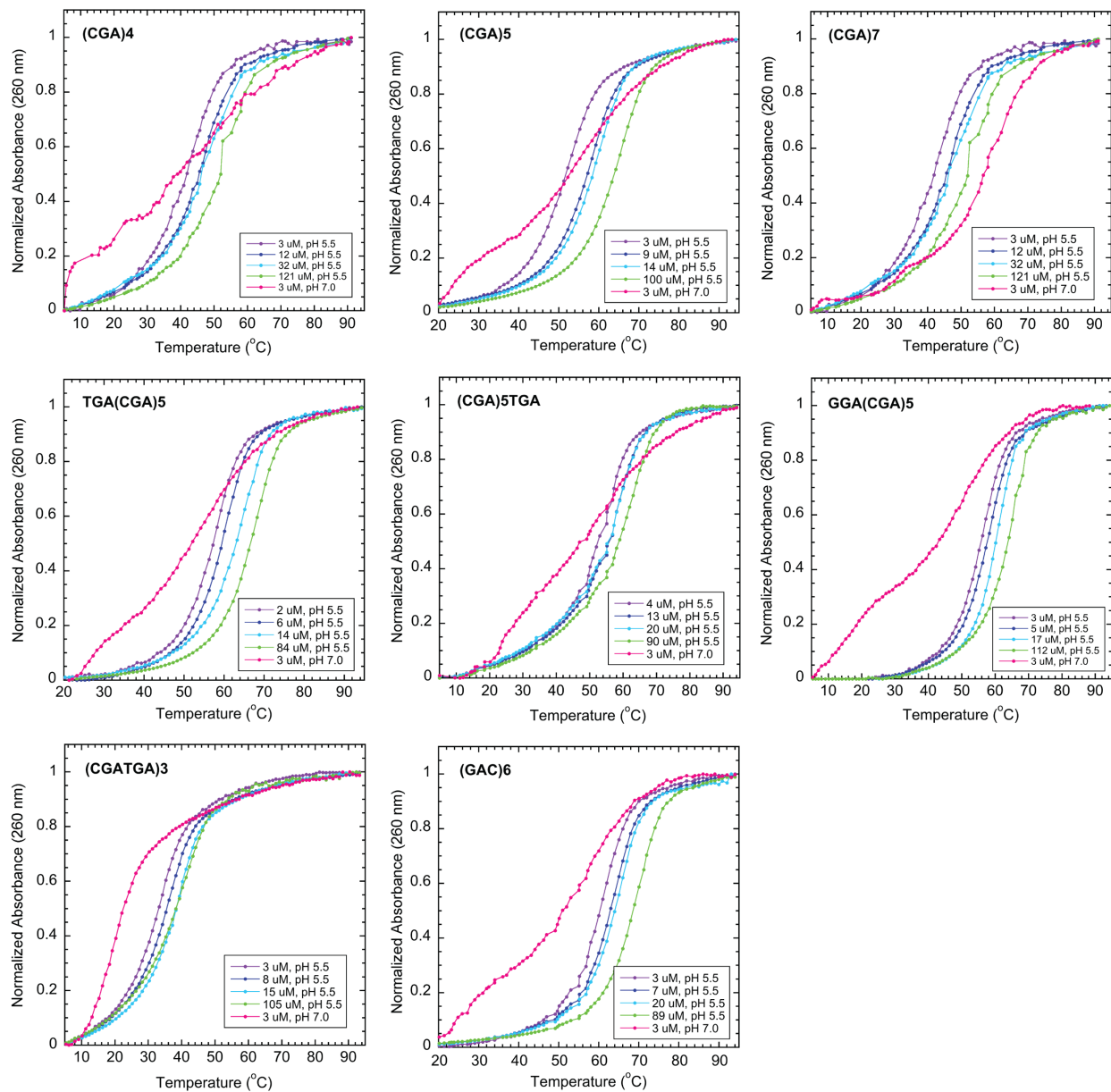


**Figure S2.** Normalized temperature versus absorbance curves for  $(CGA)_n$  variants at pH 5.5 (purple, blue, cyan, green) and pH 7.0 (pink). All  $(CGA)_n$  variants have concentration-dependent, two-state melting curves at pH 5.5, indicating bimolecular interactions. At pH 7.0, all variants exhibit non-two-state melting with apparent minor lower-temperature melting transitions between 20-40 °C.

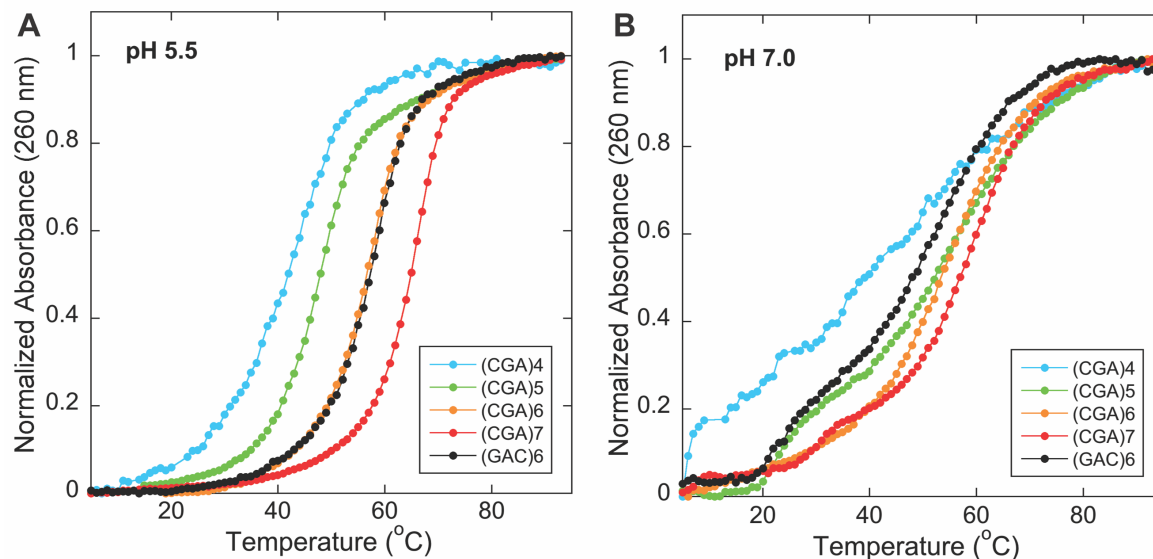


**Figure S3.** Normalized temperature versus absorbance curves for 2.5  $\mu\text{M}$   $(\text{CGA})_n$  variants, where  $n = 4$  to 7 at (A) pH 5.5 and (B) pH 7.0. It is unclear why  $(\text{GAC})_6$  behaves differently than  $(\text{CGA})_6$ , as it is a permutation of  $d(\text{CGA})$ , at pH 7.0. We suspect that the difference could arise from variations in hairpin loop and stem size, as well as the likelihood of interconversion between different hairpin forms. Assuming the  $d(\text{CGACG})$  loop is the most stable hairpin form,  $(\text{CGA})_6$  could form a 6-bp stem where the  $d(\text{CGACG})$  loop is capped by A-A producing the two-state transition seen at pH 7.0. The slight destabilization seen for  $(\text{GAC})_6$  could arise from a similar hairpin with a  $d(\text{CGACG})$  loop but only accommodating 5-bp. Further, the non-two state melt suggests that  $(\text{GAC})_6$  could be dynamically interconverting between two different forms – one with a 5-bp stem and a  $d(\text{CGACG})$  loop or 7-bp stem and a  $d(\text{ACGA})$  loop.



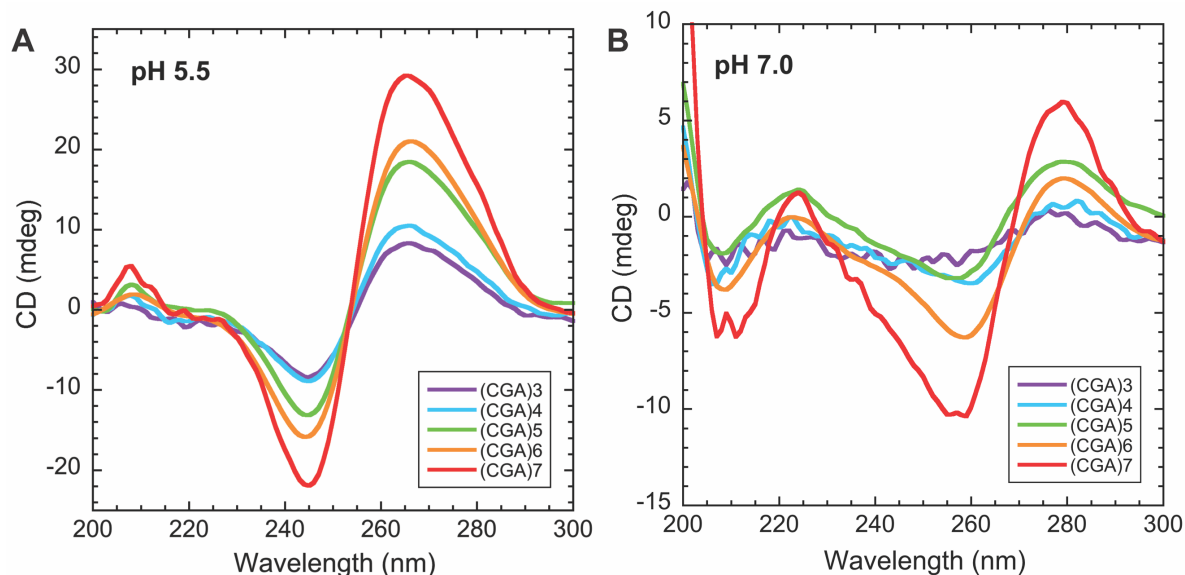


**Figure S4.** CD spectra of 10  $\mu\text{M}$   $(\text{CGA})_n$  where  $n = 3$  to 7 at (A) pH 5.5 and (B) pH 7.0. At pH 5.5, the intensity of the bands characteristic of the parallel-stranded duplex (245 nm, 265 nm) decrease as the number of d(CGA) units decrease. This suggests that the parallel-stranded form can exist at all repeat sizes tested. At pH 7.0, the signal intensity corresponding to anti-parallel strands (258 nm, 275 nm) decreases with repeat number, but is lost when  $n \leq 4$  suggesting that the hairpin structure cannot form at low repeat number.

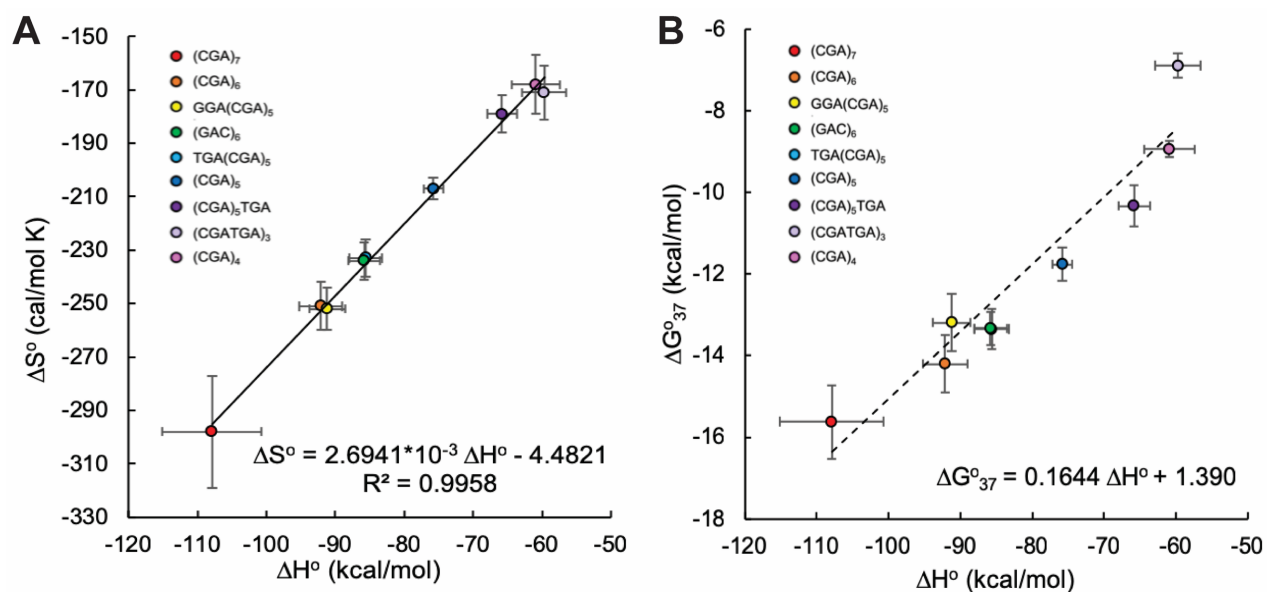


**Figure S5.** Apparent entropy-enthalpy compensation of all (CGA)<sub>n</sub> variants used in this study. **(A)** The positive correlation between  $\Delta H^\circ$  and  $\Delta S^\circ$  indicates a strong enthalpy-entropy compensation for all oligonucleotides tested. **(B)** The  $\Delta G^\circ_{37}$  vs  $\Delta H^\circ$  plot suggests that compensation is due to the underlying physical reality, as opposed to experimental error.

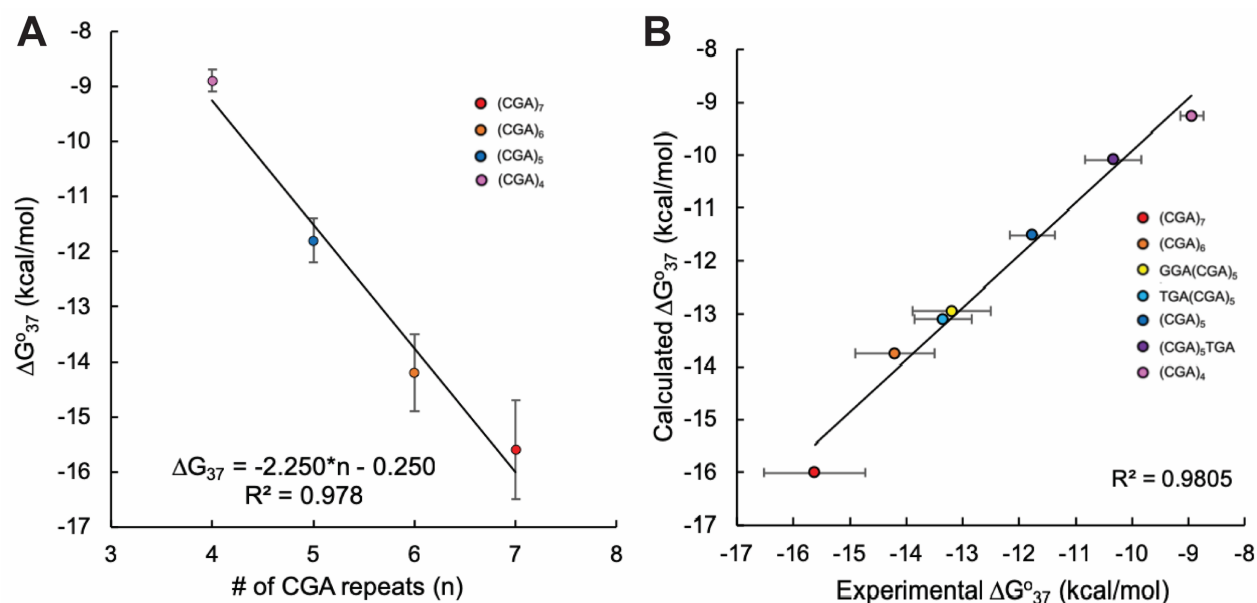


**Figure S6.** Thermodynamic estimates can be used to predict  $\Delta G_{37}^{\circ}$  values for new triplet repeat sequences. **(A)** Linear fit of  $(CGA)_n$  sequences vs experimentally obtained  $\Delta G_{37}^{\circ}$  values. **(B)** Experimental  $\Delta G_{37}^{\circ}$  is highly correlated to calculated  $\Delta G_{37}^{\circ}$  for all sequences, assuming additive contributions from each triplet. Estimates for d(CGA) were obtained from the fit in **A**, while estimates for 5'-d(GGA), 5'-d(TGA), 3'-d(TGA) were obtained from Table 1. All sequences were included except  $(TGA)_6$  and  $(CGATGA)_3$ .

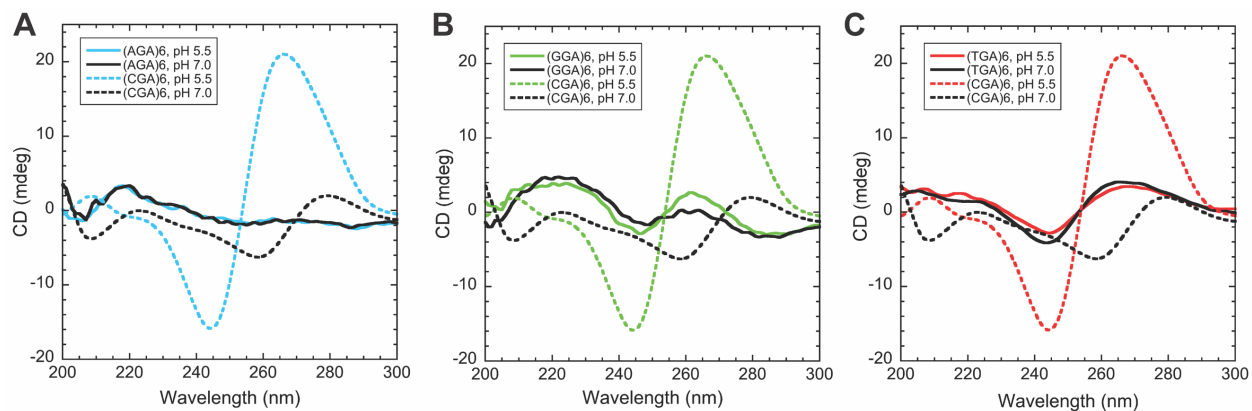


**Figure S7.** CD spectra of 10  $\mu\text{M}$  (NGA)<sub>6</sub> sequences compared to (CGA)<sub>6</sub>. **(A)** (AGA)<sub>6</sub> does not have CD bands characteristic of parallel- or anti-parallel oriented strands and is not pH dependent. The lack of CD signal could suggest a lack of structure at each pH. **(B)** (GGA)<sub>6</sub> also does not have CD bands characteristic of parallel- or anti-parallel oriented strands and is not pH dependent. The band at 220 nm could indicate the formation of a different structure at each pH. **(C)** (TGA)<sub>6</sub> has CD signal characteristic of the anti-parallel form at each pH, suggesting a lack of pH sensitivity.

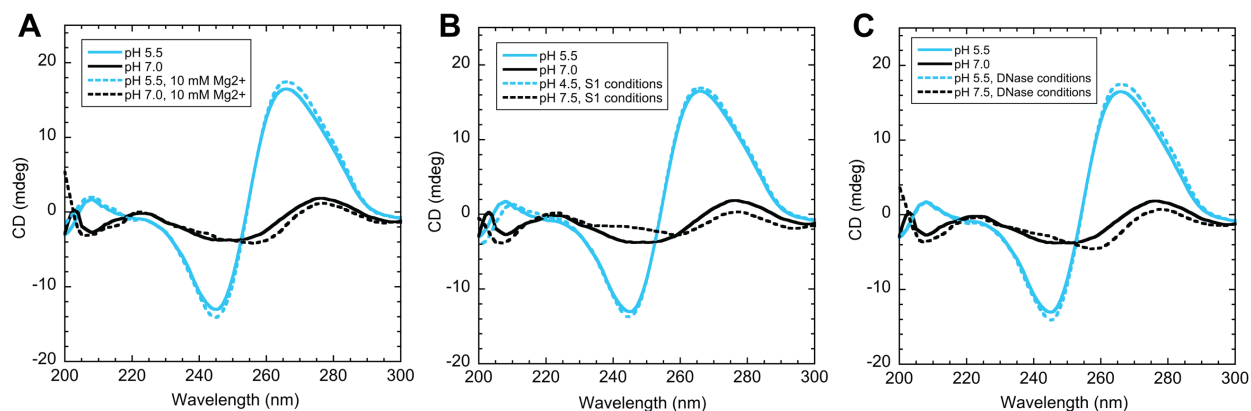


**Figure S8.** CD spectra of 10 μM GGA(CG A)<sub>5</sub> with various divalent cations at pH 5.5 (blue) and pH 7.0 (black). Divalent cations (Mg<sup>2+</sup>, Zn<sup>2+</sup>, and Ca<sup>2+</sup>) do not affect the parallel-stranded structure formed at pH 5.5 or anti-parallel structure formed at pH 7.0. (A) The addition of 10 mM magnesium chloride does not affect the structure of GGA(CG A)<sub>5</sub> at pH 5.5 or 7.0. (B) GGA(CG A)<sub>5</sub> retained parallel-stranded structure at pH 4.5 and anti-parallel structure at pH 7.5 in S1 nuclease reaction conditions containing 2 mM zinc sulfate and 300 mM sodium chloride. (C) GGA(CG A)<sub>5</sub> retained parallel-stranded structure at pH 5.5 and anti-parallel structure at pH 7.5 in DNase I nuclease reaction conditions containing 0.5 mM calcium chloride and 2.5 mM magnesium chloride.

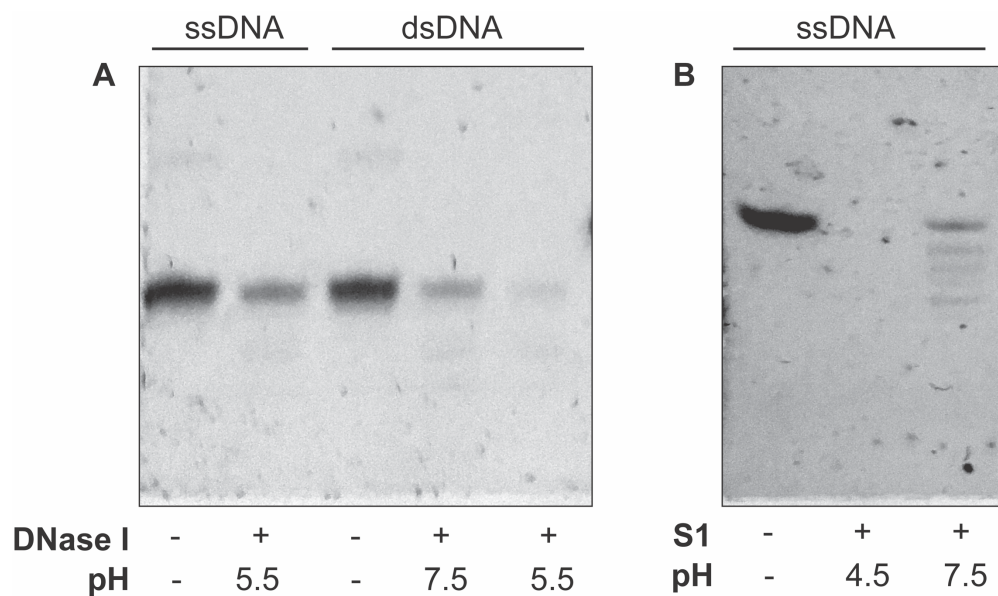


**Figure S9.** Control DNase I and S1 nuclease sensitivity experiments performed on d(GGACAGCTGGGAG) with  $Mg^{2+}$  to form double stranded (ds) DNA or without  $Mg^{2+}$  for single stranded (ss) DNA. **(A)** ssDNA and dsDNA exposed to DNase I at pH 5.5 and 7.5. DNase I functioned optimally on dsDNA at pH 5.5. Reduced activity was observed for ssDNA at pH 5.5 and dsDNA at pH 7.5. **(B)** Control ssDNA incubated with S1 nuclease at pH 4.5 and 7.5. S1 nuclease was more active at pH 4.5 than at pH 7.5.

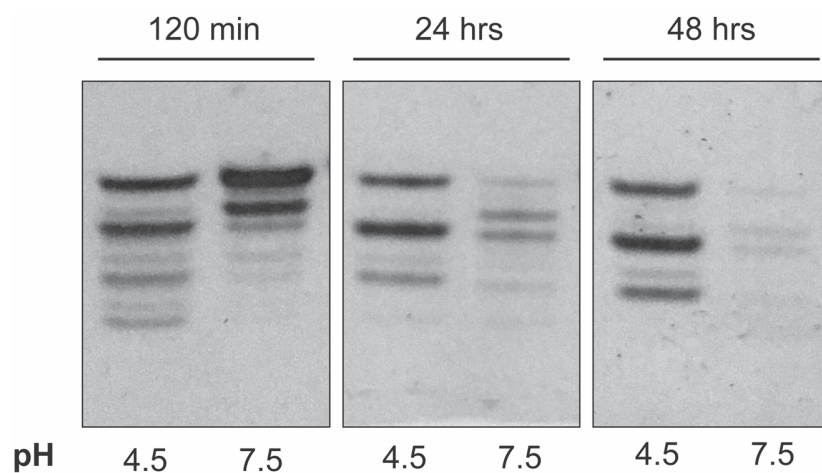


**Figure S10.** Extended S1 digestion of TGA(CG A)<sub>5</sub>. The bands are almost completely digested at pH 7.5 when TGA(CG A)<sub>5</sub> was exposed to S1 nuclease for 2 days, suggesting that the structure formed at this pH is dynamic or not resistant to S1 digestion over time. In contrast, the intensity of the 18, 15, and 12-nt bands corresponding to digestion by S1 nuclease at pH 4.5 does not change over two days of exposure. This suggests that the parallel-stranded duplex formed is stable and resistant to S1 degradation at room temperature.

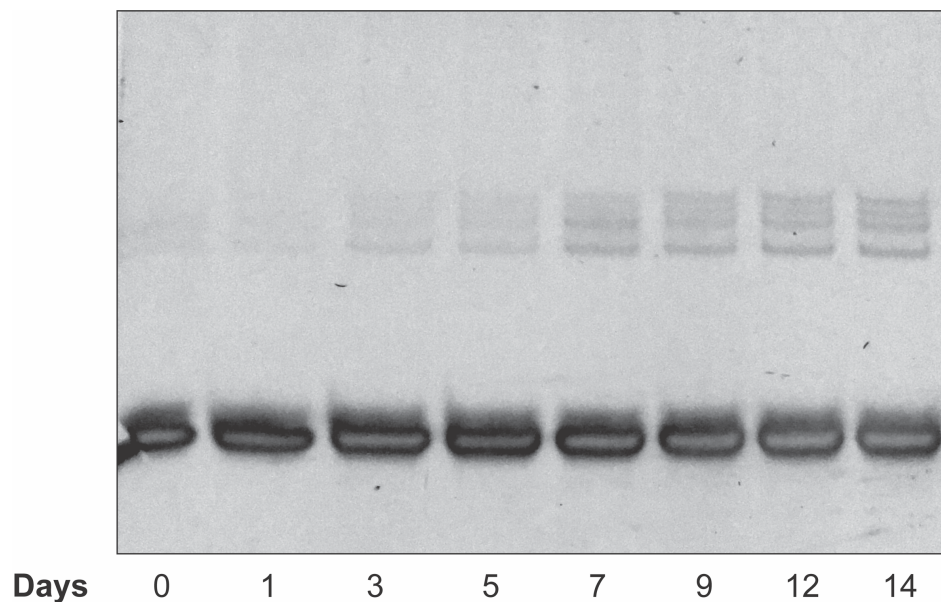


**Figure S11.** High molecular weight (HMW) bands formed over time when  $(CGA)_6$  is incubated in deionized water, at room temperature, for up to 2 weeks, as shown by denaturing PAGE. All variants, except  $(TGA)_6$ , contain HMW bands in 8 M urea denaturing gels (not shown). HMW band formation increases with time, lower pH, storage temperature and oligonucleotide concentration.